Dominant roles of the polybasic proline motif and copper in the PrP23-89-mediated stress protection response

Cathryn L. Haigh[1,2], Simon C. Drew[1,2,3,4], Martin P. Boland[1,2], Colin L. Masters[2,5], Kevin J. Barnham[1,2,3], Victoria A. Lawson[1,2] and Steven J. Collins[1,2,*]

[1]Department of Pathology, The University of Melbourne, 3010, Australia
[2]Mental Health Research Institute, The University of Melbourne, 3010, Australia
[3]Bio21 Molecular Science and Biotechnology Institute, The University of Melbourne, 3010, Australia
[4]School of Physics, Monash University, Clayton, 3800, Australia
[5]Centre for Neuroscience, The University of Melbourne, 3010, Australia
*Author for correspondence (e-mail: stevenjc@unimelb.edu.au)

Accepted 10 January 2009
Journal of Cell Science 122, 1518-1528 Published by The Company of Biologists 2009
doi:10.1242/jcs.043604

Summary

Beta-cleavage of the neurodegenerative disease-associated prion protein (PrP) protects cells from death induced by oxidative insults. The beta-cleavage event produces two fragments, designated N2 and C2. We investigated the role of the N2 fragment (residues 23-89) in cellular stress response, determining mechanisms involved and regions important for this reaction. The N2 fragment differentially modulated the reactive oxygen species (ROS) response induced by serum deprivation, with amelioration when copper bound. Amino acid residues 23-50 alone mediated a ROS reduction response. PrP23-50 ROS reduction was not due to copper binding or direct antioxidant activity, but was instead mediated through proteoglycan binding partners localised in or interacting with cholesterol-rich membrane domains. Furthermore, mutational analyses of both PrP23-50 and N2 showed that their protective capacity requires the sterically constraining double proline motif within the N-terminal polybasic region. Our findings show that N2 is a biologically active fragment that is able to modulate stress-induced intracellular ROS through interaction of its structurally defined N-terminal polybasic region with cell-surface proteoglycans.

Supplementary material available online at
http://jcs.biologists.org/cgi/content/full/122/10/1518/DC1

Key words: Prion, N-terminus, Oxidative stress, Beta-cleavage, GAG, Copper

Introduction

Prion diseases are transmissible neurodegenerative disorders causally linked to abnormal conformers (termed PrP^{Sc}) of the cellular prion protein (PrP^{C}). The role of PrP^{C} within the cell has proved difficult to resolve, with suggested functions including copper homeostasis and trafficking, signal transduction, cellular adhesion and attenuation of oxidative stress (Brown and Besinger, 1998; Brown et al., 1999; Schmitt-Ulms et al., 2001; Spielhaupter and Schätzl, 2001; Stuermer et al., 2004). Protection against oxidative stress or reactive oxygen species (ROS) has been proposed to be enzymatic, wherein PrP^{C} itself would have superoxide dismutase-like activity (Brown et al., 2001), or alternatively, mediated by signal transduction cascades, whereby the resultant reaction protects the cell (Watt et al., 2005). The regions of PrP^{C} involved in such protection have been investigated and both the C- and N-termini have been determined to be involved (Rambold et al., 2008).

The C-terminal amyloidogenic region has been more widely studied than the N-terminal region due to its propensity to misfold and so have a more prominent association with disease. However, mutations within the N-terminus are found in hereditary prion diseases, consisting of insertions or deletions within the copper-binding octameric repeat domain (Kovács et al., 2005). The N-terminal region, although not constituting part of the amyloid core of PrP^{Sc}, is thought to be biologically active, associated with clathrin-mediated internalisation and intracellular trafficking of PrP^{C} (Nunziante et al., 2003; Shyng et al., 1995; Sunyach et al., 2003), and with PrP^{C} movement at the cell surface (Taylor et al., 2005). In particular, the most N-terminal amino acids of PrP^{C} are highly conserved across mammalian species (Wopfner et al., 1999) and contain a polybasic domain (residues 23-28) shown to function as a glycosaminoglycan (GAG)-binding site (Pan et al., 2002). PrP^{C} binding to cellular receptors, including low density lipoprotein receptor-related protein 1 (Parkyn et al., 2008) and the 37 kDa/67 kDa laminin receptor (Gauczynski et al., 2001), involves the N-terminal region. Further, the latter of these PrP receptors requires heparan sulphate to mediate binding and has additionally been shown to be involved in the internalisation of PrP^{Sc} (Morel et al., 2005; Gauczynski et al., 2006).

PrP cleavage fragments, corresponding to two internal cleavage sites, can be detected in both cell culture systems and brain tissue. In non-disease states the α-cleavage fragments (N1/C1) usually have a higher prevalence than the β-cleavage fragments (N2/C2). The latter cleavage fragments are increased in the brains of Creutzfeldt-Jakob Disease (CJD) patients and mice generated as models of prion disease (Chen et al., 1995; Yadavalli et al., 2004). This increase has mainly been considered a pro-pathogenic event, but equally might represent a neuronal protective response, attempting to compensate for increased stress during disease progression. Consistent with this hypothesis, cell lines expressing mutant PrP species that do not undergo N2/C2 cleavage are rendered unable

to respond to oxidative stress insults (Watt et al., 2005). Further studies have shown that, in the context of full-length PrP, tethering the N-terminus abolishes protective responses against various cellular stressors (Dupiereux et al., 2008; Zeng et al., 2003).

The enigmatic nature of the hereditary disease-associated, highly conserved N-terminal region of PrP^C prompted us to look more closely at its function. Our specific aim was to elucidate if and how the N-terminal β-cleavage product (N2) of the prion protein modulates intracellular ROS under conditions of enhanced stress. Copper co-ordination of a representative murine N2 fragment, encompassing residues 23-89, favourably influenced intracellular ROS produced in response to serum deprivation. The most N-terminal region (23-50), independent of copper coordination, also conferred a cellular protective effect resulting in reduced intracellular ROS. This effect was shown to be dependent on cell-surface, heparan-sulphate-containing proteoglycans, which are either localised to, or require interaction with, lipid-raft domains. Furthermore, the two proline residues within the polybasic region at the N-terminus of mature PrP^C (residues 26 and 28) were found to exert a dominant effect over the cellular association of this region and the redox-protective activity of PrP23-89.

Results

N2 differentially modulates the production of intracellular ROS in response to serum deprivation depending on copper occupancy

β-Cleavage of PrP^C is reportedly ragged. Amino acid 89 was selected for the C-terminal residue, as this approximates the mid-point of the β-cleavage range (Fig. 1A) and ensures that the octapeptide repeat domain is intact, which is likely to be important for the biological functions of N2. To investigate potential protective effects, PrP23-89 was applied to CF10 cells manifesting increased intracellular ROS. CF10 cells were the primary cell line used in this study, as they represent a PrP^C-null background to avoid potentially confounding effects caused by the activity of full-length PrP, the complementary C2 fragment or endogenously produced N2. Cellular ROS insults were induced using serum deprivation to avoid the peptides contacting serum proteases that might degrade them. Intracellular ROS levels were assayed using the DCFDA assay, which detects H_2O_2 (in the presence of endogenous metal ions), $HO^{\cdot}$, $ROO^{\cdot}$, and $ONOO^-$ (Martin et al., 1998). The ROS generated and viability data in response to decreasing serum concentrations are shown in supplementary material Fig. S1. When applied in a $\log_{10}$ dilution series from 0.01-10,000 nM the N2 fragment increased the intracellular ROS in serum-deprived CF10 cells to a plateau at 1 nM peptide (Fig. 1B,C). By contrast, when 10 μM peptide was applied with equimolar followed by 2-6 molar equivalents of $CuCl_2$-6×glycine, a protective effect compared with 'no peptide', 'peptide' and 'copper alone' treatments was seen from 2-4 molar equivalents (Fig. 1B,D). One to six molar equivalents (10–60 μM) of copper alone showed progressively increasing ROS up to 5 equivalents and a lesser effect at 6 equivalents; the latter effect is most likely due to a reduction in cell viability caused by copper toxicity. A peptide corresponding to the amino acid sequence of PrP23-89 scrambled was also assayed and showed no variation from baseline ROS production in response to serum deprivation or serum deprivation with 1-6 molar equivalents of $CuCl_2$-6×glycine (supplementary material Fig. S2).

PrP23-50 attenuates the intracellular ROS response

To explore the PrP domains responsible for the activity of the N2 fragment, a peptide encompassing only the copper-binding octameric repeat domain (PrP51-89) and an N-terminal peptide lacking this domain (PrP23-50) were employed. These were applied to the CF10

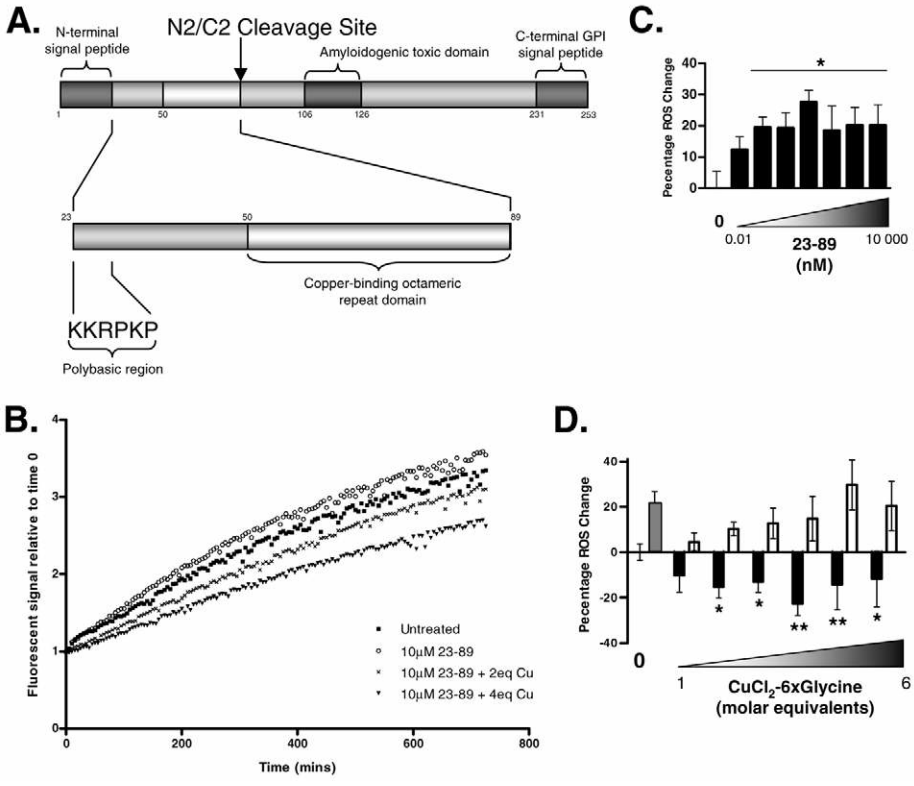

Fig. 1. PrP23-89 (N2) modulates intracellular oxidative stress conditional upon copper saturation. (A) Schematic representation showing the defined regions of PrP and the approximate internal cleavage site producing N2 and C2 fragments. (B-D) N2 reduces ROS induced by serum deprivation only when pre-loaded with copper. Synthetic N2 encompassing murine amino acids 23-89 was applied to serum-deprived CF10 cells in a $\log_{10}$ serial dilution from 0.01-10,000 nM. The 10,000 nM concentration was also applied after pre-mixing with 1-6 molar equivalents of copper; 1-6 equivalents of copper were applied without peptide for comparison. (B) Example of intracellular ROS curves obtained using the DCFDA fluorescent dye. Initial rates were calculated as the linear tangent to the curve and are shown as the percentage change from the baseline rate obtained for the serum-free environment. (C) ROS rate changes induced by the apo-PrP23-89 peptide over the dilution series. Significantly increased intracellular ROS production is seen from 0.1 nM peptide (one-way ANOVA, F=11.22, P=0.001, *P<0.01). The effect of copper-loading the PrP23-89 peptide on intracellular ROS is shown in D, with black bars indicating the copper-loaded peptide and white bars indicating the equivalent copper-alone condition. For comparison, the grey bar shows the intracellular ROS response to the peptide alone. Conditions significantly different from both the copper- and peptide-alone controls, as determined by two-way ANOVA (F=45.49, P<0.001), are indicated by *P<0.05 **P<0.01.

cells in the same $\log_{10}$ serial dilution as used for PrP23-89 and, as 51-89 is a characterised copper-binding domain, the PrP51-89 peptide was also applied with 1-6 equivalents of $CuCl_2$-6×glycine. PrP51-89 showed increased intracellular ROS at low concentrations and with 1-3 equivalents of $CuCl_2$ (Fig. 2A), whereas the PrP23-50 fragment decreased the intracellular ROS produced by serum deprivation at the lowest concentration used (0.01 nM), significant at 10 nM peptide (Fig. 2B). To check for specificity of the PrP23-50 reaction, a scrambled peptide corresponding to the amino acid composition of PrP23-50 (PrP23-50scram) was also assayed and showed no significant ability to decrease (or increase) the intracellular ROS produced by serum deprivation (Fig. 2B).

Neuro2a cells show copper-dependant PrP23-89 ROS reduction and PrP23-50 ROS reduction at higher peptide concentrations

Wild-type PrP-expressing cells are likely to be influenced by endogenous expression of full-length PrP and the N2/C2 cleavage fragments. However, to ascertain whether a response could still be elicited by increased N2 at the membrane, Neuro2a (N2a) cells were exposed to 10 μM PrP23-89 with and without 4 molar equivalents $CuCl_2$-6×glycine. Both the apo PrP23-89 and the copper-loaded peptide were able to reduce intracellular ROS in response to serum deprivation, with the copper-loaded PrP23-89 showing a lesser response than the apo PrP23-89 (Fig. 3A). The reason for such a discrepancy most likely arises from the basal copper content of the cells, as the brains of null mice have been shown to have reduced copper concentrations compared with their wild type counterparts (Brown, 2003). To confirm this we incubated the cell lines with the copper-reactive fluorescent dye Phen Green Fl, which is quenched by both Cu^+ and Cu^{2+} and also has a lesser reactivity with iron and cobalt (Chavez-Crooker et al., 2001). This confirmed greater basal metal ion concentrations in the N2a cells compared with the CF10 cells (Fig. 3B). The N2a cells showed no response to the PrP51-89 fragment (Fig. 3A); however, when PrP23-50 was assayed by dose titration, there was a specific and significant ROS reduction at 1 μM peptide (Fig. 3C). This is a higher concentration than seen for the CF10 cells and most likely indicates that the endogenous PrP is exerting an effect that mutes the reaction. As shown for the CF10 cells, the response of the N2a cells to decreasing serum concentrations and to PrP23-89scram are included in supplementary material Figs S1 and S2, respectively.

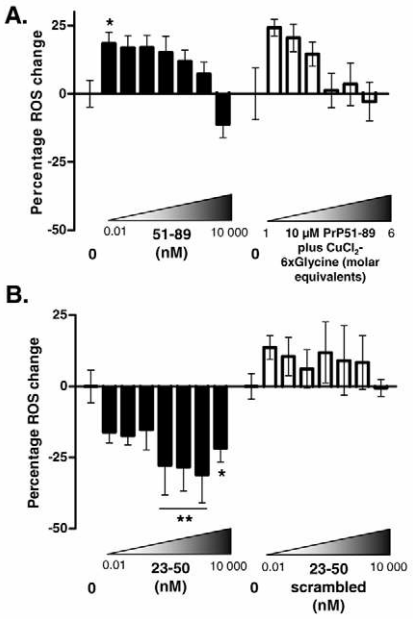

Fig. 2. Amino acids PrP23-50 alone reduce the ROS response to serum deprivation. Synthetic PrP51-89 and PrP23-50 were added to serum-deprived cells in the $\log_{10}$ serial dilution from 0.01-10,000 nM and the intracellular ROS response measured by DCFDA assay (A and B, black bars). PrP51-89 (10 μM) was also assayed with 1-6 molar equivalents $CuCl_2$-6×glycine (white bars). Changes in the rate of ROS production are represented as the percentage change from the rate induced by serum deprivation alone. PrP51-89 at 0.01 nM and when loaded with 1-2 molar equivalents $CuCl_2$-6×glycine shows no significant difference from when copper alone is applied (two-way ANOVA; F=1.225, P=0.2738). Cells treated with PrP23-50 show significantly reduced intracellular ROS in response to serum deprivation from 10-10,000 nM peptide (one-way ANOVA; F=4.774, P=0.0018, *P<0.05, **P<0.01). To eliminate the possibility of non-specific effects, a scrambled peptide (PrP23-50scram) was also assayed (B; white bars). No significant change in the rate of ROS production is seen for the PrP23-50scram peptide (one-way ANOVA, F=0.4482, P=0.8615).

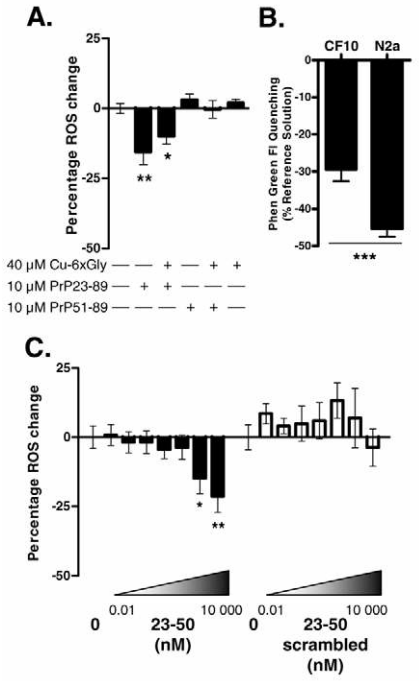

Fig. 3. Wild-type N2a cells show ROS reduction in response to PrP23-89 and PrP23-50. (A) PrP23-89 and PrP51-89 (10 μM) were added to N2a cells with and without 4 molar equivalents of $CuCl_2$-6×glycine and assayed for the ROS produced in response to serum deprivation by the DCFDA assay. Changes in the rate of ROS production are represented as the percentage change from the rate induced by serum deprivation alone. PrP23-89 both with and without copper significantly reduced the intracellular ROS induced by serum deprivation (one-way ANOVA F=6.298, P=0.0021, *P<0.05, **P<0.01). (B) Phen green quenching experiments show that N2a cells have higher basal concentrations of copper compared with CF10 cells (Student's t-test, t=4.148, **P=0.0025), possibly explaining the ROS-reducing activity of apo PrP23-89 in these cells compared to that seen in the CF10 cells. (C) PrP23-50 (black bars) and PrP23-50scram (white bars) were added to serum-deprived cells in the $\log_{10}$ serial dilution from 0.01-10,000 nM. Cells treated with PrP23-50 show significantly reduced intracellular ROS in response to serum deprivation from 1000-10,000 nM peptide (one-way ANOVA, F=4.774, P=0.0018, *P<0.05, **P<0.01). No significant change in the rate of ROS production is seen for the PrP23-50scram peptide (one-way ANOVA, F=0.4482, P=0.8615).

PrP23-50 does not mediate its protective response by copper binding or direct antioxidant activity

Although the octameric repeat copper-binding domain has been well characterised, the PrP23-50 region has been less rigorously investigated. To clarify how this fragment mediates the intracellular ROS reduction effect, we investigated its ability to coordinate copper or to directly act as an antioxidant molecule. Electron paramagnetic resonance (EPR) spectroscopy indicated that both PrP23-50 and PrP23-50scram were able to coordinate copper upon addition of 1 molar equivalent of $CuCl_2$; however, both peptides readily surrendered their copper load to 2.5 molar equivalents of the weak copper chelator glycine (Fig. 4A). This indicates that the copper binding of PrP23-50 is non-specific at pH 7.0 (K_d>1 μM) and unlikely to be biologically meaningful in the cell-protective effect. When PrP23-50 and PrP23-50scram were assayed for their ability to reduce ROS produced by the Fenton reaction, with the radicals produced detected by fluorescent spin trapping, neither peptide showed any antioxidant ability (Fig. 4B). Circular dichroism (CD) spectroscopy confirmed that PrP23-50 adopts a predominantly random coil structure, indistinguishable from that of PrP23-50scram, indicating that the assumption of altered secondary structure in the absence of the octameric repeat domain is unlikely to be relevant to the PrP23-50 ROS reduction effect (Fig. 4C).

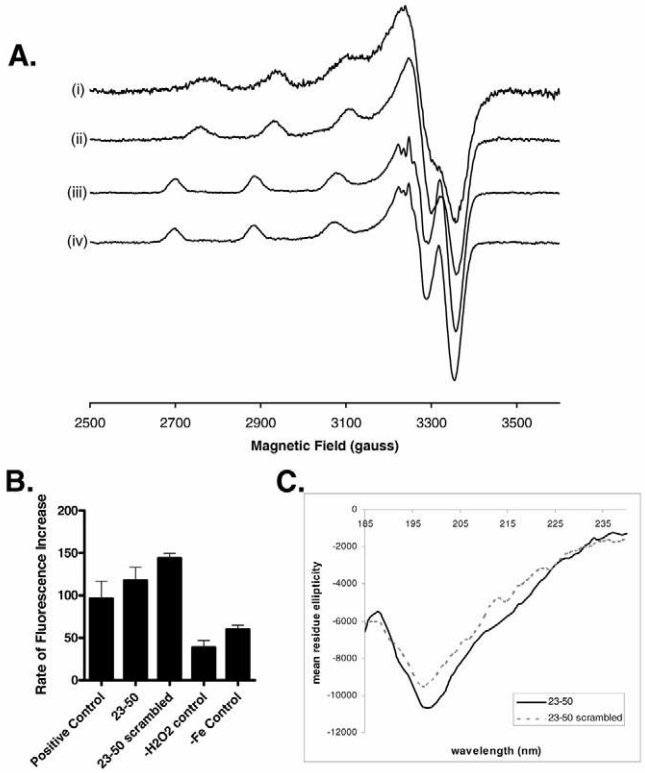

Fig. 4. The PrP23-50 region has limited copper-binding ability, is not an antioxidant and assumes no specific secondary structure. (A) EPR spectra of PrP23-50 (i,iii) and PrP23-50scram (ii,iv) with 1 molar equivalent of Cu^{2+} in the absence (i,ii) and presence (iii,iv) of 2.5 molar equivalents glycine. Both peptides readily surrender their bound copper to the low-affinity chelator glycine, indicating that PrP23-50 binds copper non-specifically like any unstructured peptide, with the N-terminal amine, backbone amide(s) and water molecules being the likely ligands. The principal $g_{||}$ and $A_{||}$ parameters characterising the spectra ($g_{||}$~2.23, $A_{||}(^{65}Cu)$~170-180×$10^{-4}cm^{-1}$) are compatible with a 3N1O or 2N2O coordination sphere of equatorial ligands. Spin quantification by double-integration of the spectra indicates that PrP23-50 and PrP23-50scram bind around 1/3 and 1/2, respectively, of the observable Cu^{2+} bound in the presence of glycine; the unbound Cu^{2+} fraction forms EPR-silent copper hydroxide at pH 7 (Drew and Barnham, 2008). (B) The ability of PrP23-50 to act as an antioxidant was assessed by response to the Fenton reaction caused by H_2O_2 and $FeSO_4$, with the fluorescent radical trap proxyl fluorescamine used to capture hydroxyl radicals produced. In comparison with the positive control, neither PrP23-50 nor PrP23-50scram showed any ability to reduce the radicals reaching the trap. Shown are the mean rates with s.e.m. for three independent experiments. (C) CD spectroscopy shows that both PrP23-50 and PrP23-50scram adopt a predominantly random coil structure.

PrP23-50 mediates its intracellular ROS-attenuating effect through a proteoglycan binding partner found within, or requiring, intact cholesterol-rich domains

In the absence of a direct biochemical explanation for the ROS reduction response of PrP23-50, cellular interactions were investigated. First trypsin was used to crudely remove all cell-surface protein and the production of intracellular ROS induced by serum deprivation monitored by the DCFDA assay as before with and without PrP23-50 applied in the log_{10} serial dilution. Trypsinising the cells did not significantly alter the rate of ROS produced in the absence of serum (Fig. 5A, left panel), but the PrP23-50 fragment no longer significantly reduced ROS levels (Fig. 5A, right panel), indicating that the PrP23-50 response most likely involves a protein-binding partner as opposed to lipid-membrane interactions. Filipin III complex, an antibiotic that binds and sequesters cholesterol, was used to disrupt cholesterol-rich lipid-raft domains within the cell membrane. Lipid-raft domains are known to be important signalling platforms, and so potential binding partners may reside in, or mediate their response through, resident proteins. Treatment with filipin III showed a trend toward a reduced ROS rate in response to serum deprivation in the absence of peptide, but this was not significant (Fig. 5B, left panel). Filipin III-treated cells showed no response to any concentration of the PrP23-50 fragment, indicating that lipid-raft domains are involved in mediating the PrP23-50 ROS reduction response (Fig. 5B, right panel). The transferrin receptor, which is excluded from lipid-raft domains, was used as a control to show preserved location of non-raft proteins (supplementary material Fig. S3).

The most N-terminal amino acids of PrP23-50 contain a polybasic GAG-binding site. Therefore to more closely examine the nature of a PrP23-50-binding partner, two GAG-catabolising enzymes were used to selectively remove cell-surface GAGs of interest from their protein cores. Cells were treated with heparin lyase III to remove heparan sulphate or chondroitinase ABC to remove chondroitin A, B and C, and were then assayed for their intracellular ROS response to serum deprivation with and without addition of the log_{10} dilution of PrP23-50. The removal of GAGs by both enzymes induced a significant increase in intracellular ROS production in response to serum deprivation (Fig. 5C,D, left panels): however, the chondroitinase ABC-treated cells were still receptive to reduction of intracellular ROS by PrP23-50 (Fig. 5D, right panel). The heparin lyase III-treated cells showed no reduction in ROS when incubated with PrP23-50 (Fig. 5C, right panel), indicating that the PrP23-50 response is dependant on proteoglycans containing heparan sulphate. The effective removal of over 40% of cellular heparan sulphate was confirmed by dot blotting, as shown in supplementary material Fig. S4.

The PrP octarepeat domain, with and without bound copper, influences N-terminal peptide cell association or internalisation and half life

The N-terminal polybasic region (amino acids 23-28) has been shown to be essential for PrP^C internalisation (Sunyach et al., 2003).

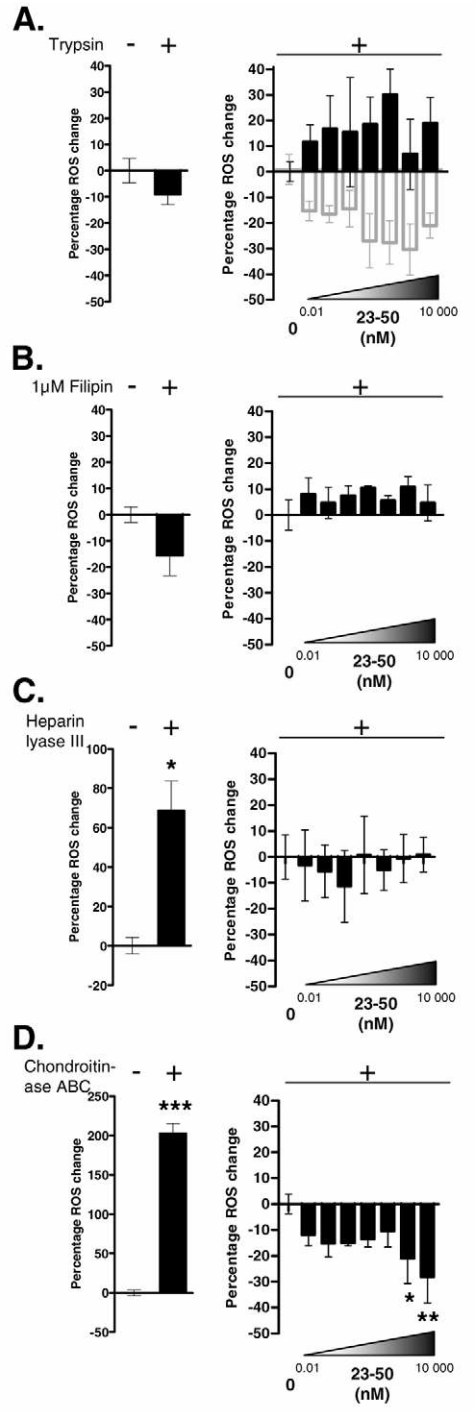

Fig. 5. Removal of cell membrane proteins or heparan sulphate, or disruption of lipid rafts, abolishes the PrP23-50-mediated intracellular ROS reduction response to serum deprivation. The effect of the cell surface environment on the protective function of PrP23-50 against intracellular ROS was assessed using the DCFDA assay. The $\log_{10}$ serial dilution of PrP23-50 was applied to the cells after treatment with (A) trypsin before the start of the assay, (B) 1 μM filipin III for the duration of the assay, (C) heparin lyase III at 10 mU/ml for 1 hour before the start then at 5 mU/ml for the duration of the assay, and (D) chondroitinase ABC as for the heparin lyase III treatment. For each condition the left panel shows the effect of the treatment on the production of intracellular ROS compared with serum-free media only, and the right panel shows the effect of the PrP23-50 peptide on the cells after they have been exposed to the treatment. Alterations in the rate of ROS production before PrP23-50 treatment have been compensated for in the analysis. The results of PrP23-50 treatment (in the absence of other treatment) are shown as empty grey bars in panel A for comparison. Significant results as determined by Student's *t*-test for changes in the rate caused by the treatment or by one-way ANOVA for changes induced by PrP23-50 are indicated by $*P<0.05$, $**P<0.01$ and $***P<0.001$.

Therefore, to address whether the PrP23-50 effect might be a result of internalisation by its protein-binding partner(s), cells were treated for 0-60 minutes with 10 μM peptide (PrP23-50 alone and PrP23-89 with/without 4 molar equivalents $CuCl_2$-6×glycine) and both cell lysates and media western blotted for the peptides. Peptide within the cell lysate fraction may be internalised or membrane-bound (referred to as 'cell-associated'). The strongest cell-associated signal was seen in cells treated with PrP23-89 without copper. Even 1 minute post-exposure the peptide can be seen clearly within this fraction and already seems to have reached its plateau (Fig. 6A,B). When PrP23-89 is applied pre-loaded with copper, the initial signal is much weaker and increases over time to an overall lower level. This indicates that in the absence of copper the octarepeats can mediate binding to the cell surface and/or internalisation, which is disconnected to protection against intracellular ROS, whereas when copper is bound the octarepeat site is less cell-accessible or binding becomes more specific. PrP23-50 shows almost no cell association, indicating that low levels of cell association are sufficient to achieve protection or that the response must be the result of a rapid, transient linkage. When the rate of disappearance of PrP23-50 from the media and the overall rate of disappearance of the fragment are considered (Fig. 6C,D), PrP23-50 is seen to disappear much faster than the PrP23-89 peptide (with or without copper), indicating that PrP23-50 is turned over much more rapidly. Rapid destruction at the membrane or within the cell may explain the lack of PrP23-50 signal within the cell-associated fraction. Copper binding to PrP23-89 appeared to slow the overall loss of this peptide, possibly as a result of more gradual binding to its cellular partners at the membrane, resulting in a slower catabolic processing.

Mutational analysis of the N-terminal polybasic region indicates that proline residues 26 and 28 are required for specific interaction and generation of the intracellular ROS protective effect

It has previously been shown that the internalisation response of PrP^C is diminished if the positively charged amino acids of the N-terminal polybasic region are mutated to more neutrally charged residues (Sunyach et al., 2003). The charge of this region, however, is not its only feature. Within the charged residues are two prolines: a motif that functionally is highly significant. Proline motifs are known to impart a degree of structure onto proteins due to the steric constraints of the rigid pyrrolidine ring (reviewed by Vanhoof et al., 1995). Proline motifs are very often found in association with positively charged amino acids, and therefore we hypothesised that these two proline residues were likely to be an essential part of the functional moiety and crucial for the biological activity of PrP23-50 and PrP23-89. To test this hypothesis, the PrP23-50 fragment was synthesised with prolines 26 and 28 mutated to alanine. Alanine was substituted for proline because of its similar size and charge properties but lack of rigid structure. The ability of PrP23-50 P26/28A to reduce the ROS induced by serum deprivation in the CF10 cells was tested using the $\log_{10}$ serial dilution of peptide. The PrP23-50 P26/28A peptide showed no ability to modulate intracellular ROS induced by serum deprivation (Fig. 7A). Furthermore, when cell lysates and media were probed to look for internalisation/cell association it was

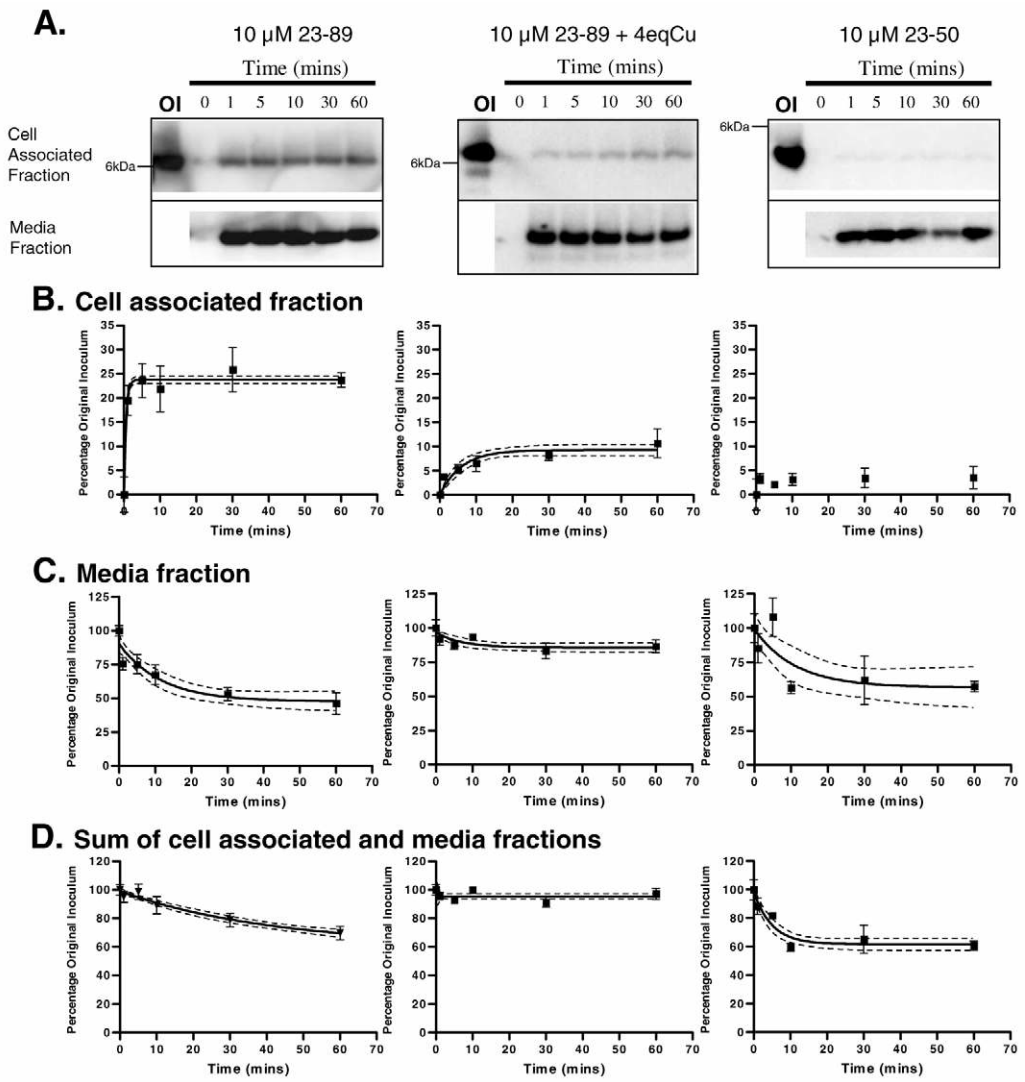

Fig. 6. The octarepeat region modulates cellular association and peptide turnover. 10 µM of the PrP23-89 fragment with and without premixing with 4 molar equivalents of $CuCl_2$-6×glycine, and the PrP23-50 fragment were added to cells at 0 (background control) to 60 minutes. After this time cell lysates and media were harvested and western blotted to detect the fragments. (A) Example blots showing the cell-associated (upper plate) and media (lower plate) fractions compared to the original inoculums (OI). Band signals were quantified densitometrically and the signal represented as a percentage of the OI signal. Graphs show the mean and s.e.m. of (B) the cell-associated fraction, (C) the media fraction and (D) the sum of both fractions as an indicator of total loss of the peptide from the system, derived from three independent experiments. Where appropriate the single exponential rate curves for association or decay are shown (unbroken line) with the 95% CI (broken lines). Copper binding reduces the rate of cellular association of the PrP23-89 fragment and the intensity once association has reached equilibrium, but also reduces its loss from the media and the overall system. The PrP23-50 fragment shows almost no cellular association but a rapid, overall greater loss from the media and the system than the PrP23-89 fragment, even when the latter is not copper-bound.

shown that this mutation enhanced signal in the cell-associated fraction (Fig. 7B,C). Complementary to the increase in cell association, a rapid decrease in the culture medium and in the overall detected peptide was observed (Fig. 7D,E). Additionally the peptide displayed altered physical properties, now showing a tendency to aggregate, with both the monomer and the aggregates showing cell association (Fig. 7B). CD spectroscopy, however, did not reveal any overt alteration in secondary structure from that of wild-type PrP23-50 (supplementary material Fig. S5).

Proline residues 26 and 28 exert a dominant influence over the properties of N2

To determine the importance of the proline residues within the polybasic region of the N2 fragment on the intracellular ROS protective activity and, further, if the polybasic region could exert a dominant effect over the octarepeat region, PrP23-89 with the P26/28A mutations was synthesised. The production of intracellular ROS in response to serum withdrawal was assessed in the presence of PrP23-89 P26/28A with and without copper as described for wild-type PrP23-89. When applied to the serum-deprived cells without pre-loading with copper, minimal variation was seen from baseline in the rate of ROS production up to 1 µM peptide, where the tendency is toward increased ROS production as seen for PrP23-89 (Fig. 8A). When PrP23-89 P26/28A was applied with equimolar, followed by 2-6 molar equivalents of $CuCl_2$-6×glycine, a pronounced difference was seen from PrP23-89 (Fig. 8B). One to three equivalents of copper induced a sizable increase in the rate of ROS production compared with copper alone or the PrP23-89

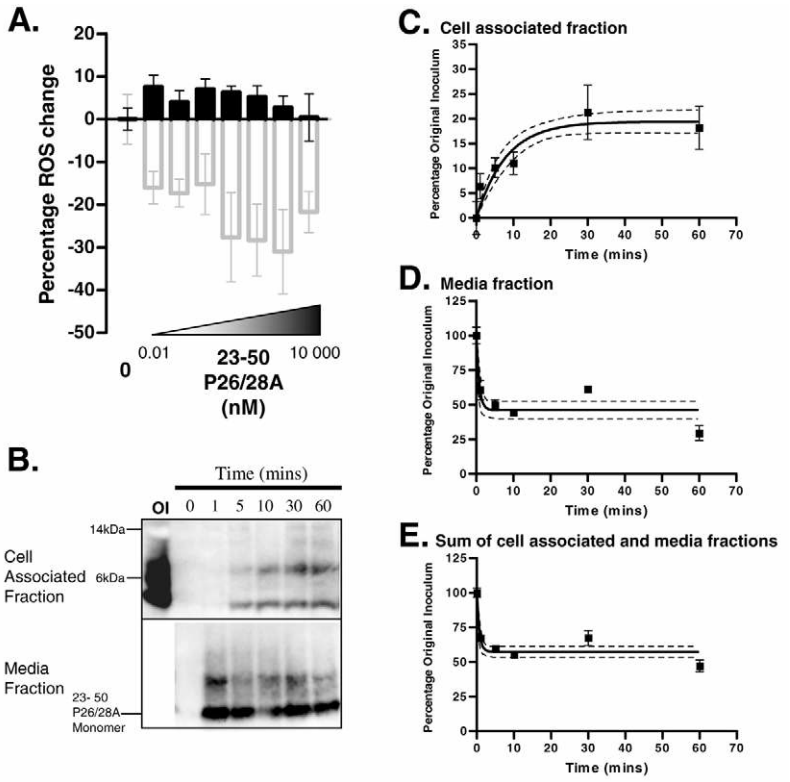

Fig. 7. Mutation of the proline residues 26 and 28 to alanine abolishes the activity of PrP23-50 and alters its cellular association. PrP23-50 was synthesised with proline residues 26 and 28 mutated to alanine. (A) Percentage changes in the rate of ROS production from the rate induced by serum deprivation alone as determined by DCFDA assay for the $\log_{10}$ serial dilution of the PrP23-50 P26/28A fragment (black bars), the PrP23-50 fragment results are shown for comparison (empty grey bars). 10 μM of the PrP23-50 P26/28A fragment was added to cells at 0 (background control) to 60 minutes. Cell lysates and media were harvested and western blotted to detect the fragment. (B) Example blots showing the cell-associated (upper plate) and media (lower plate) fractions compared to the original inoculum (OI). Band signals were quantified densitometrically and the signal represented as a percentage of the OI signal. Graphs show the single exponential rate curves for association or decay (unbroken line) with the 95% CI (broken lines) of (C) the cell-associated fraction, (D) the media fraction and (E) the sum of both fractions as an indicator of total loss of the peptide from the system, derived from three independent experiments. The PrP23-50 P26/28A fragment shows a greater propensity to associate with the cell than the PrP23-50 fragment and decays from the media and the overall system faster. Further it shows a tendency to aggregate, not seen for the PrP23-50 fragment.

copper-loaded fragment. Full saturation, at 4 equivalents of copper, was no different in ROS production from the cellular response seen for this concentration of copper alone. Five to six equivalents of copper was not significantly different from the PrP23-89 response. As the increased intracellular ROS seen at the lower equivalents of copper may have been a result of cellular toxicity by the peptide delivering copper into the cell, an MTS assay for cell viability was performed on the cells 24 hours after treatment (Fig. 8C). Significantly reduced viability was seen at the 2 equivalent copper concentration for cells treated with the PrP23-89 P26/28A fragment, but no significant difference in viability was seen at 1 equivalent, where the highest ROS were seen or at any of the higher concentrations of copper. Cells were treated for 0-60 minutes with the apo or copper-loaded PrP23-89 P26/28A and lysates and media western blotted for the presence of the fragment as described previously. Like the PrP23-50 P26/28A, the PrP23-89 P26/28A fragment showed increased tenancy to aggregate compared with the wild-type PrP23-89 (Fig. 8D,E), with two dominant oligomeric forms evident. When a 4 molar excess of copper was premixed with the PrP23-89 P26/28A fragment the oligomers were reduced, with the monomer band becoming the dominant species (Fig. 8D,F). This suggests that mutating the N-terminal prolines to less structurally constraining amino acids allows the octarepeats to associate with each other, forming aggregates sensitive to copper binding. This, however, is not the only region responsible for the aggregation, as the PrP23-50 P26/28A fragment without the octapeptide repeats aggregates and oligomeric species remain in the copper-loaded sample. The dominant aggregated species in the unloaded sample shows the greatest propensity to internalise, with the monomer showing much less cellular association; this is reversed in the cell fraction treated with the copper-loaded peptide. Cell association and rate of disappearance from the media curves are shown in supplementary material Fig. S6. Overall, the eventual cellular association concentration plateau of copper-loaded PrP23-89 P26/28A is no greater than that of copper-loaded wild-type PrP23-89. However, at 1 minute post-exposure, only approximately 4% of the copper-loaded PrP23-89 was associated with the cellular fraction, whereas approximately 15% of the copper loaded PrP23-89 P26/28A was seen in this fraction. This rate of cellular association may place cells under extra stress, resulting in the increased ROS seen in these treatments. Alternatively, the increased oxidative stress seen when cells are exposed to this fragment may be due to a mis-association of the fragment or the remaining oligomeric species. Furthermore, despite the differences in intracellular ROS production when PrP23-89 P26/28A was applied with 1 molar equivalent copper, EPR data on the binding of 1 molar equivalent copper shows there was no difference in copper coordination between the PrP23-89 and PrP23-89 P26/28A fragments, and CD spectra confirm there were no significant differences in secondary structure (Fig. 8G; Fig. 7H).

Discussion

β-Cleavage of the prion protein occurs internally around the C-terminal end of the octameric repeat domain (Chen et al., 1995) and has been shown to protect against ROS induced by copper and hydrogen peroxide (Watt et al., 2005). Our results significantly extend this knowledge by showing that the N-terminal β-cleavage product specifically modulates intracellular ROS occurring in response to cellular stress, with the protection mediated by both its copper-binding and non-copper-binding regions. Further, copper saturation facilitated the attenuation of intracellular ROS concomitant with altered cellular association properties of the N2 peptide. Hence, differences in intracellular ROS between cells treated with the apo-N2 and the copper-loaded-N2 peptide are very likely due to different interactions at the cell membrane. The PrP octameric repeat domain has been shown to bind to membranes in

model systems and the addition of copper to this region, although still allowing binding, changed the conformational arrangement (Dong et al., 2007). A change in peptide conformation, peptide-lipid orientation or peptide position in relation to the cell membrane may allow the far N-terminal residues to interact with differing binding partners, or at different locations on the cell membrane, resulting in distinct cellular responses. This is not the case for the PrP23-50 fragment, which, without the octarepeat domain, is free to interact directly with its binding partners independent of any stress-sensing or modulating role of copper binding. Proposed models of N2 interactions with itself and the lipid membrane environment are depicted schematically in Fig. 9B.

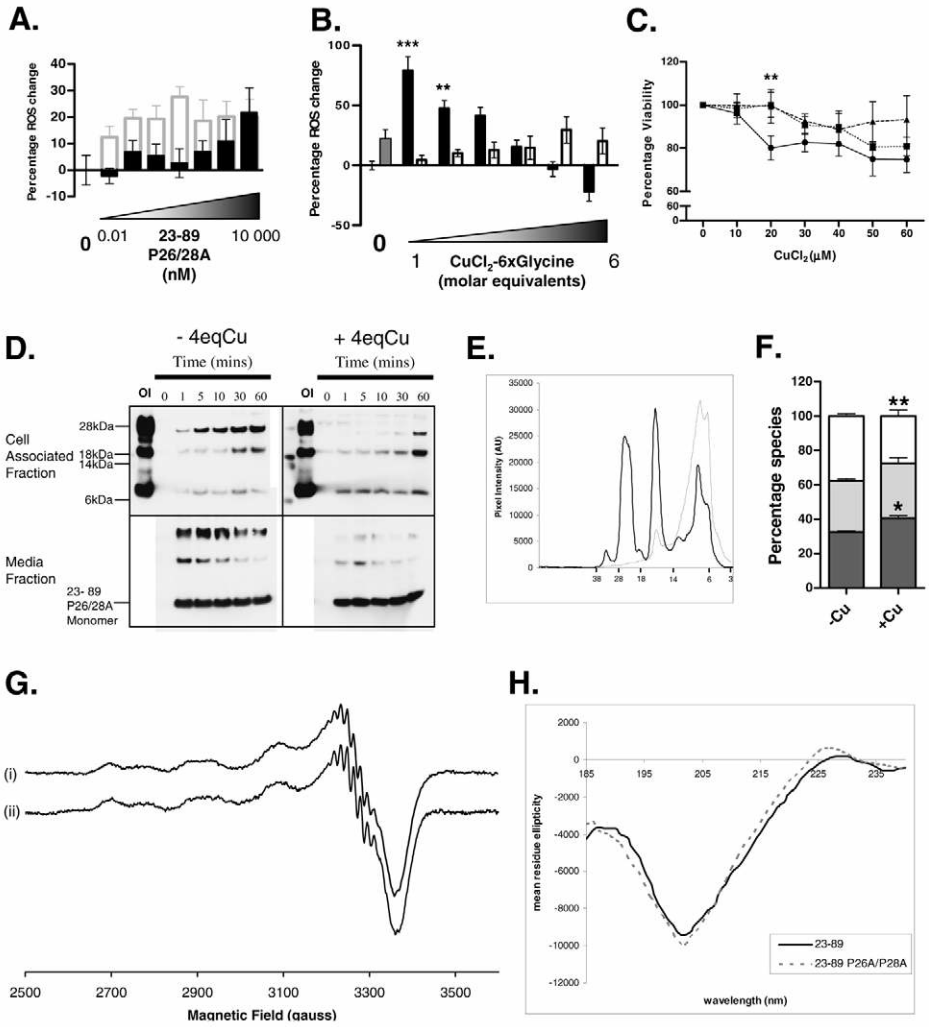

Fig. 8. Mutation of the polybasic region prolines results in altered properties of PrP23-89. The PrP23-89 fragment was synthesised with prolines 26 and 28 mutated to alanine. The ability of this peptide to modulate the ROS response to serum deprivation with and without copper loading was monitored by DCFDA assay. All plots represent the mean and s.e.m. of four independent experiments, except panel F, where n=3. (A) The apo-23-89 P26/28A fragment was applied to cells in the $\log_{10}$ serial dilution. The ROS response compared with cells not exposed to the peptide is shown (black bars) in comparison to the PrP23-89 peptide response (empty grey bars). (B) Intracellular ROS response to serum depletion when applying 10 µM peptide with 1-6 molar equivalents $CuCl_2$-6×glycine (black bars), compared with the response of the peptide alone (grey bar) and the response of $CuCl_2$-6×glycine alone (white bars). Two-way ANOVA finds that the change in ROS rate at 1 and 2 equivalents copper are significantly different from the results obtained for wild-type PrP23-89 (F=14.74, P<0.0001, **P<0.01, ***P<0.001). (C) Viability of cells treated with 10 µM PrP23-89 P26/28A peptide and increasing equivalents of copper for 24 hours (circles and solid line) expressed relative to the no-copper condition, and compared with equivalent wild-type PrP23-89 (triangles and dashed line) and copper alone (squares and dotted line). Decreased viability is seen for the PrP23-89P26/28A peptide against both PrP23-89 and copper alone at 2 equivalents copper and relative to just the PrP23-89 peptide at 5 and 6 equivalents of copper (F=4.83, P=0.0422, *P<0.05, **P<0.01). (D) Cells were treated for 0 (background control) to 60 minutes with 10 µM PrP23-89 P26/28A with and without 4 molar equivalents of $CuCl_2$-6×glycine. Cell-associated and media fractions were western blotted for the presence of the PrP23-89 P26/28A fragment compared with the original inoculum (OI). (E) Densitometric profiles measured vertically from the top to the bottom of the PrP23-89 P26/28A (solid line) and the wild-type PrP23-89 (dashed line) original inoculums. The PrP23-89 P26/28A fragment showed enhanced aggregation compared to the wild-type PrP23-89, with several dominant species appearing. (F) Densitometric quantification of the three most dominant species in the original inoculum lanes expressed as a percentage of their sum indicates copper saturation induces a shift from the dominant upper band (white bar segments) to increased dominance of the middle (pale grey bar segments) and monomeric bands (dark grey bar segments). Changes in the upper and monomeric band intensities are significant by two-way ANOVA (F=7.018, P=0.0269, *P<0.05, **P<0.01). (G) EPR spectra of (i) PrP23-89 and (ii) PrP23-89 P26/28A in the presence of 1 molar equivalent $^{65}CuCl_2$ at pH 7.0. Multiple coordination modes exist in equilibrium for PrP23-89 that are very similar to those of isolated octapeptide repeat fragments at physiological pH (Drew and Barnham, 2008). These are unchanged upon mutation of prolines 26 and 28 to alanines. The co-ordination observed in PrP23-50 (Fig. 3A) does not occur here due to the higher affinity of the octarepeat copper coordination modes. (H) CD spectra show that the mutation of the proline residues does not alter secondary structure.

The N-terminal polybasic region has previously been shown to be crucial for internalisation of PrP^{C}; this was dependent on its strong positive charge (Nunziante et al., 2003; Sunyach et al., 2003). In the current study the polybasic region was also involved in the ROS reduction response, requiring the proline residues 26 and 28 within this charged region. Proline residues induce small structural motifs due to the steric constraints imposed by their rigid cyclic structure. It is probable that the charge of the 23-28 polybasic region mediates N2 binding to proteoglycans and the structure imparted on the N-terminus by the double proline motif produces the selectivity of this reaction. The net result is specific recognition of target-binding partners most likely within the cholesterol-rich lipid-raft domains in which PrP^{C} is resident. Mutation of the prolines within the polybasic region, producing a less rigid N-terminus, permitted the N2 peptide to interact more readily with the cell while simultaneously abolishing its specific protective properties and producing potentially deleterious effects. This was exemplified by the PrP23-89 P26/28A ROS response in the presence of copper. Here, cellular association was significantly increased compared with the wild type PrP23-89 fragment, indicating that the mutant peptide probably moves copper inside the cell or to an incorrect membrane location, causing increased cellular stress at low concentrations of copper.

Among many other functions, proteoglycans can be cellular receptors and co-receptors (reviewed by Raman et al., 2005). The specific function of the proteoglycan is determined by its protein core. PrP^{C} has several putative GAG-binding sites that might differentially mediate binding to proteoglycans, which are located at amino acid positions PrP23-50, 53-93 and 110-128 (Warner et al., 2002). The GAGs bound by cell-free recombinant PrP include heparin, heparan sulphate, chondroitin sulphate A and B, hyaluronic acid and dextran (Andrievskaia et al., 2007; Pan et al., 2002), and cellular PrP expressed by transfection binds heparin (Pan et al., 2002). Heparan sulphate has been shown to be a cell surface receptor for PrP^{Sc} (Horonchik et al., 2005) and preincubation of infectious inoculum with heparin delays the onset of prion disease (Hijazi et al., 2005), indicating that uptake of PrP^{Sc} can be decreased by exogenous GAGs competing with endogenous GAGs. Furthermore GAGs mediate PrP^{C} binding to cell-surface receptors including the 37 kDa/67 kDa laminin receptor (Gauczynski et al., 2001). The regions involved in 37 kDa/67 kDa laminin receptor binding have been characterised and the N2 fragment and the octameric repeats alone, in the presence of heparan sulphate, can bind to and are outcompeted by antibodies against the laminin receptor (Hundt et al., 2001). Receptor binding such as this may transduce the ROS protective effect seen in response to the PrP N-terminus in this study; this is depicted in Fig. 9C.

Copper binding to the octameric repeat domain alters GAG binding (Andrievskaia et al., 2007; Warner et al., 2002). Increased octarepeats, as seen in some genetic prion diseases, increases the binding capacity and affinity for GAGs, and both increased repeats and increased GAG binding decrease the ability of the cell to respond to ROS (Yin et al., 2006; Yin et al., 2007). Moreover, increased GAG binding is associated with increased aggregation of full-length PrP (Yin et al., 2007), and aggregation of PrP is also associated with a decreased response to oxidative stress. These observations are consistent with those reported here, wherein altering the two N-terminal prolines resulted in enhanced cellular association and increased aggregation but with a concomitant loss of the protective response against intracellular ROS. Further, the current data support a biologically meaningful role for GAG binding in the protective function of the N-terminus, and identify the importance of structure within the polybasic region in addition to any electrostatic contributions to this interaction. By contrast, aberrant association with the cell membrane could induce an intracellular ROS insult, which might potentially contribute to the pathogenesis of prion disease.

The cellular location of the β-cleavage event has not yet been established; however the N-terminus has been shown to be important

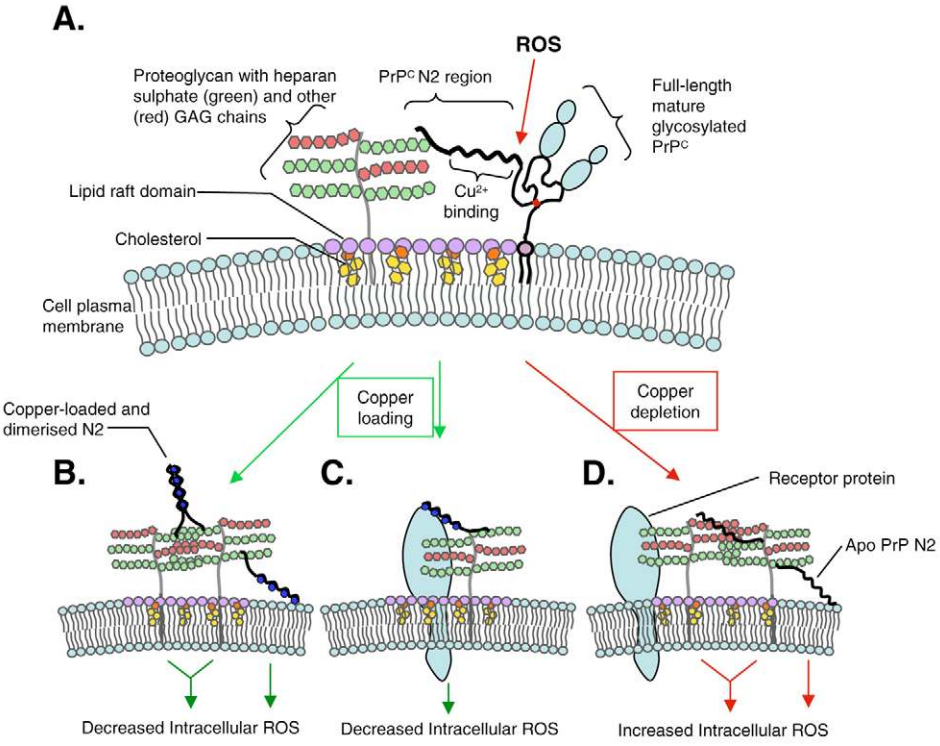

Fig. 9. Scheme depicting hypothetical modes of action of the N2 fragment. It is probable that the flexible N-terminus is bound to GAGs via the polybasic region even when resting at the cell membrane (A). Upon release of the N2 region by ROS the fragment is free to instigate further interactions. As N2/C2 cleavage most likely occurs when the octarepeats are already occupied to some extent with copper, new interactions might include metal-ion induced dimerisation of N2 fragments (B) or, as the octarepeats also bind lipids, coordination with GAGs and the lipid membrane environment, also transducing a protective effect via lipid signalling pathways. An alternative result of N2/C2 cleavage might be to deliver the N2 fragment to a cell-surface receptor such as the laminin receptor (Gauczynski et al., 2001), where binding to the receptor could initiate a protective signal transduction cascade (C). In the event the N2/C2 cleavage occurs when copper levels are depleted or if the fragment was outcompeted for copper by another protein, different interactions may occur with GAGs or with the lipid membrane environment, preventing the N2 fragment from interacting with the appropriate receptor and resulting an unrelated, possibly detrimental signal (D).

in mediating protective effects from the cell surface. Tethering of the N-terminus of full-length PrP to the membrane effectively prevented PrP-mediated protection against ROS insults induced by hydrogen peroxide (Zeng et al., 2003) and paraquat (Dupiereux et al., 2008). In the current study synthetic N-terminal fragments were added exogenously to the extracellular surface to investigate stress protection mediated from outside the cell. Given that PrP^{C} is an extracellular cell-surface protein and that both N-terminal (N1 and N2) cleavage fragments have been found in higher concentrations in conditioned medium than within cell lysates (Mangé et al., 2004; Vincent et al., 2001), with the N2 fragment increased especially after treatment with hydrogen peroxide and copper (McMahon et al., 2001), it is reasonable to assume that at least part of the N-terminal function is mediated from the outer leaflet of the cell membrane. Rapid degradation following internalisation of these fragments may explain their higher prevalence in the extracellular environment. This is common for peptide ligands that activate signal transduction pathways, because prolonged signalling can result in activation of detrimental cellular pathways, including apoptosis (reviewed by Junttila et al., 2008). The rapid turnover of signalling ligands probably explains the lack of PrP23-50 detected in cell lysate, as without the octarepeat region its effects are more potent than the N2 fragment, so it must be removed before its presence becomes harmful to the cell. Further experiments will reveal whether production of the N2 fragment inside the cell can initiate a differing effect from that seen when it is produced at the cell surface, or whether interaction with the complementary C2 and/or full-length PrP^{C} can modulate function.

β-Cleavage of PrP is increased during disease, as evidenced by increased N2/C2 cleavage products in the brains of CJD patients and in the brains of scrapie-infected mice (Chen et al., 1995; Yadavalli et al., 2004). ROS markers, such as lipid peroxidation, are also linked with early stages of prion disease (Brazier et al., 2006). The β-cleavage event is caused by ROS (McMahon et al., 2001; Watt et al., 2005), and furthermore, an inability to undergo β-cleavage renders the cell susceptible to oxidative attack (Watt et al., 2005). Impaired β-cleavage is seen for certain disease-associated PrP mutations, including expansion of the octameric repeat region (Watt et al., 2005). Cells expressing PrP mutations with increased repeats are more susceptible to oxidative-stress-induced cellular damage and death (Watt et al., 2005; Watt et al., 2007). Taken together, this indicates that the β-cleavage event is unlikely to be an irrelevant epiphenomenon of PrP^{C} to PrP^{Sc} conversion but, instead, part of a cellular response to stress that is compromised by certain pathogenic mutations.

Overall, the current study has shown that through binding to extracellular proteoglycans, in association with lipid-raft domains, the N-terminus of PrP^{C} is active in favourably modulating intracellular ROS changes caused by cellular stress. Further, we postulate that the octapeptide repeat, through variable copper binding, may function as a biosensor for activation of the protective N2 region, with the structure and charge specificity of the polybasic domain ensuring the correct transducing receptor engagement.

Materials and Methods

Cell culture

Reagents were purchased from Invitrogen (VIC, Australia) unless otherwise stated. CF10 (murine neuronal PrP knockout) cells and Neuro2a (N2a) cells were cultured in Dulbecco's modified Eagle's media supplemented with 10% (v/v) fetal bovine serum and 50 U/ml penicillin/50 µg/ml streptomycin solution (Sigma). Cells were maintained at 37°C with 5% CO_2 in a humidified incubator. For microtitre plate assays, cells were plated to be 90-95% confluent at the start of the assay.

Preparation of synthetic peptides

The following synthetic peptides based on the N-terminal sequence of murine PrP – (23)KKRPKPGGWNTGGSRYPGQGSPGGNRYP(50)PQGGTWGQPHGGGWG-QPHGGSWGQPHGGSWGQPHGGGWGQ(89) – were purchased from the peptide synthesis unit of the Bio21 Institute (Victoria, Australia), which uses microwave-assisted peptide synthesis; PrP23-89; PrP23-50; PrP23-50 P26/28A; PrP23-89 P26/28A; PrP23-50scram (GKPWSGRGTPGGRGPRKYGSNKYRNGPQ); and PrP23-89scram (KQSQYGGGPSWGNYWGWPGHGRGPGPRGQPGGTRGPGG-TQSWKPGGGHWPSGGHQGGPKHWGQNPGG). Peptides were solubilised in distilled water before addition to cell culture media with concentrations determined by UV spectroscopy.

DCFDA assay

Cells were incubated in Dulbecco's phosphate-buffered saline (dPBS) containing 5 µM 5-(and-6)-chloromethyl-2′,7′-dichlorodihydrofluorescein diacetate, acetyl ester (CM-H_2-DCFDA) at 37°C for 20 minutes, then probe solution was removed and replaced with prewarmed Opti-MEM I Reduced-Serum Medium (without phenol red) with or without test reagent added. Readings were taken every 5 minutes for 12 hours using 490 nm excitation and 520 nm emission filters in a Fluostar Optima (BMG Labtech, Victoria, Australia), and initial rates were calculated using tangents to the curve.

Phen Green Fl assay

Cells were incubated in prewarmed Opti-MEM I Reduced-Serum Medium (without phenol red) containing 10 µM Phen green FL diacetate for 20 minutes and residual cellular fluorescence compared with the cell-free control solution. Readings were taken using 490 nm excitation and 520 nm emission filters in a Fluostar Optima.

Cell viability (MTS) assay

Five µl of one solution MTS reagent per 100 µl media (Promega; VIC AUS) was added to test and medium-only background control conditions, and incubated under normal culture conditions for 90 minutes. Reaction product was quantified using absorbance at 462 nm in a Fluostar Optima.

GAG digestion

Cells were digested for 1 hour at 37°C in OptiMEM1 culture media using 10 mU/ml of heparin lyase III or chondroitinase ABC (Seikagaku, Japan) before the start of each assay. The enzyme concentration was reduced to 5 mU/ml during the assay. Negative controls were treated identically except for omission of the enzyme.

Circular dichroism

CD spectra were recorded at room temperature on a Jasco J-815 spectropolarimeter. Peptides were solubilised in distilled water to a concentration of 10 µM. Spectra were obtained in a 2 mm path length quartz cell from 190–240 nm using a 1 nm bandwidth and a scan rate of 50 nm min^{-1}. Background correction was performed by subtraction of the protein-free spectrum.

Electron paramagnetic resonance

Peptides were solubilised in distilled water at a concentration of 100 µM. A 10 mM $^{65}CuCl_2$ stock was prepared by dissolving ^{65}CuO (Cambridge Isotope Laboratories) in concentrated HCl, followed by dilution in distilled water. From this stock, 1 equivalent ^{65}Cu was added to each peptide solution. For Cu^{2+}-binding competition studies, 2.5 equivalents glycine was further added from a fresh 10 mM stock prepared in distilled water. The final pH was measured using a micro-probe (Hanna Instruments, Italy) and adjusted to pH 7.0 using concentrated NaOH. Samples were transferred to quartz EPR tubes (Wilmad) and snap-frozen in liquid nitrogen.

X-band CW-EPR was performed using a Bruker ESP380E spectrometer fitted with a rectangular TE_{102} microwave cavity and a quartz cold finger insert. Experimental conditions were: microwave frequency, 9.42 GHz; microwave power, 10 mW; modulation amplitude, 4 G; modulation frequency, 100 kHz; temperature, 77 K; sweep time, 168 seconds; time constant, 164 milliseconds; receiver gain, 10^5; 8-15 averages. Background correction was performed by subtraction of the sample-free spectrum. Displayed spectra were normalised with respect to their maximum peak-to-peak intensity.

Fluorescent spin trapping

Of each peptide, 10 µM was incubated with 10 µM proxyl fluorescamine, 10 µM H_2O_2, 5 µM $FeSO_4$ and 5% (v/v) DMSO in PBS. Reagents were added into wells of a black microplate with the $FeSO_4$ added last. Readings were begun immediately using 360 nm excitation and 480 nm emission wavelengths in a Fluostar Optima. Assays were run over a period of two hours to collect the linear rate of radical generation. Readings were taken every 30 seconds following 5 seconds mixing.

PAGE and western blotting

Media were removed from the cells and replaced with pre-warmed Opti-MEM I Reduced-Serum Medium at the beginning of the assay. At the appropriate time point, 10 µM peptide was added to the cells and at the end of the incubation media was removed and kept for analysis. Cells were lysed in RIPA buffer [50 mM Tris-HCl pH 7.4, 150 mM NaCl, 0.1% (w/v) SDS, 0.5% (w/v) sodium deoxycholate, 1% (v/v)

NP-40] supplemented with 0.5 U/ml benzonase (Sigma Aldrich), at 37°C for 20 minutes. Lysates and media were mixed with appropriate volumes of 3× LDS loading dye (containing 5% v/v beta-mercaptoethanol), denatured for 10 minutes at 80°C and electrophoresed in MES buffer using 12% NuPAGE Bis-Tris gels, at 200V for 35 minutes, with the dye front not allowed to reach the end of the gel. Protein was then transferred onto nitrocellulose membranes (BioRad, NSW AUS) using a BioRad wet blotting system for 30 minutes at 100V, and subsequently blocked in PBS containing 0.1% v/v Tween (PBS-t) and 5% non-fat milk. Synthetic PrP fragments were detected using 1 in 10,000 dilution of 8B4 monoclonal antibody (against murine amino acids 37-44; Alicon, Switzerland) in 1% milk PBS-t, anti-mouse HRP secondary antibody (GE Healthcare, NSW AUS) was used at 1 in 10,000 dilution and blots were visualised using ECL-plus detection reagent (GE Healthcare).

Densitometry and statistical analyses

Luminescent signal of the bands on the western blots was captured using a Las-3000 intelligent darkbox (FujiFilm; Berthold, VIC AUS) and the intensity quantified, after the subtraction of background, by ImageJ 1.38×. Statistical analyses were carried out using GraphPad Prism 5 statistical software. Graphs show the mean and s.e.m. of four independent experiments unless otherwise stated.

This work was supported by an NHandMRC Program Grant #400202. C.L.H. is supported by a University of Melbourne Early Career Researcher Grant, S.J.C. by an NHandMRC Practitioner Fellowship #400183, S.J.C. and V.A.L. by an NHandMRC Project Grant #454546, and V.A.L. by an NHandMRC Project Grant #400229. K.J.B. is an NHandMRC Senior Research Fellow.

References

Andrievskaia, O., Potetinova, Z., Balachandran, A. and Nielsen, K. (2007). Binding of bovine prion protein to heparin: a fluorescence polarisation study. *Arch. Biochem. Biophys.* **460**, 10-16.

Brazier, M. W., Lewis, V., Ciccotosto, G. D., Klug, G. M., Lawson, V. A., Cappai, R., Ironside, J. W., Masters, C. L., Hill, A. F., White, A. R. et al. (2006). Correlative studies support lipid peroxidation is linked to PrP^{res} propagation as an early primary pathogenic event in prion disease. *Brain Res. Bull.* **68**, 346-354.

Brown, D. R. (2003). Prion protein expression modulates neuronal copper content. *J. Neurochem.* **87**, 377-385.

Brown, D. R. and Besinger, A. (1998). Prion protein expression and superoxide dismutase activity. *Biochem. J.* **334**, 423-429.

Brown, D. R., Wong, B. S., Hafiz, F., Clive, C., Haswell, S. J. and Jones, I. M. (1999). Normal prion protein has an activity like that of superoxide dismutase. *Biochem. J.* **344**, 1-5.

Brown, D. R., Clive, C. and Haswell, S. J. (2001). Antioxidant activity related to copper binding of native prion protein. *J. Neurochem.* **76**, 69-76.

Chavez-Crooker, P., Garrido, N. and Ahearn, G. A. (2001). Copper transport by lobster hepatopancreatic epithelial cells separated by centrifugal elution: measurements with the fluorescent dye Phen Green. *J. Exp. Biol.* **204**, 1433-1444.

Chen, S. G., Teplow, D. B., Parchi, P., Teller, J. K., Gambetti, P. and Autilio-Gambetti, L. (1995). Truncated forms of the human prion protein in normal brain and in prion diseases. *J. Biol. Chem.* **270**, 19173-19180.

Dong, S. L., Cadamuro, S. A., Fiorino, F., Bertsch, U., Moroder, L. and Renner, C. (2007). Copper binding and conformation of the N-terminal octarepeats of the prion protein in the presence of DPC micelles as membrane mimetic. *Biopolymers* **88**, 840-847.

Drew, S. C. and Barnham, K. J. (2008). Biophysical investigations of the prion protein using electron paramagnetic resonance. In *Prion Protein Protocols* (*Methods in Molecular Biology)* Vol. 459 (ed. A. F. Hill). pp. 173-196. New Jersey: Humana Press.

Dupiereux, I., Falisse-Poirrier, N., Zorzi, W., Watt, N. T., Thellin, O., Zorzi, D., Pierard, O., Hooper, N. M., Heinen, E. and Elmoualij, B. (2008). Protective effect of prion protein via the N-terminal region in mediating a protective effect on paraquat-induced oxidative injury in neuronal cells. *J. Neurosci. Res.* **86**, 653-659.

Gauczynski, S., Peyrin, J. M., Haïk, S., Leucht, C., Hundt, C., Rieger, R., Krasemann, S., Deslys, J. P., Dormont, D., Lasmézas, C. I. et al. (2001). The 37kDa/67kDa laminin receptor acts as the cell-surface receptor for the cellular prion protein. *EMBO J.* **20**, 5863-5875.

Gauczynski, S., Nikles, D., El-Gogo, S., Papy-Garcia, D., Rey, C., Alban, S., Barritault, D., Lasmézas, C. I. and Weiss, S. (2006). The 37kDa/67kDa laminin receptor acts as a receptor for infectious prions and is inhibited by polysulphated glycanes. *J. Infect. Dis.* **194**, 702-709.

Hijazi, N., Kariv-Inbal, Z., Gasset, M. and Gabizon, R. (2005). PrPSc incorporation into cells requires endogenous glycosaminoglycan expression. *J. Biol. Chem.* **280**, 17057-17061.

Horonchik, L., Tzaban, S., Ben-Zaken, O., Yedidia, Y., Rouvinski, A., Papy-Garcia, D., Barritault, D., Vlodavsky, I. and Taraboulos, A. (2005). Heparan sulphate is a cellular receptor for purified infectious prions. *J. Biol. Chem.* **280**, 17062-17067.

Hundt, C., Peyrin, J. M., Haïk, S., Gauczynski, S., Leucht, C., Rieger, R., Riley, M. L., Deslys, J. P., Dormont, D., Lasmézas, C. I. et al. (2001). Identification of interaction domains of the prion protein with its 37-kDa/67-kDa laminin receptor. *EMBO J.* **20**, 5876-5886.

Junttila, M. R., Li, S. P. and Westermarck, J. (2008). Phosphatase-mediated crosstalk between the MAPK signalling pathways in the regulation of cell survival. *FASEB J.* **22**, 954-965.

Kovács, G. G., Puopolo, M., Ladogana, A., Pocchiari, M., Budka, H. van Duijn, C., Collins, S. J., Boyd, A., Giulivi, A., Coulthart, M. et al. (2005). Genetic prion disease: the EUROCJD experience. *Hum. Genet.* **118**, 166-174.

Mangé, A., Béranger, F., Peoc'h, K., Onodera, T., Frobert, Y. and Lehmann, S. (2004). Alpha- and beta-cleavages of the amino terminus of the cellular prion protein. *Biol. Cell* **96**, 125-132.

Martin, B. D., Schoenhard, J. A. and Sugden, K. D. (1998). Hypervalent chromium mimics reactive oxygen species as measured by the oxidant-sensitive dyes 2′,7′-dichlorofluorescin and dihydrorhodamine. *Chem. Res. Toxicol.* **11**, 1402-1410.

McMahon, H. E., Mangé, A., Nishida, N., Créminon, C., Casanova, D. and Lehmann, S. (2001). Cleavage of the amino terminus of the prion protein by reactive oxygen species. *J. Biol. Chem.* **276**, 2286-2291.

Morel, E. Andrieu, T., Casagrande, F., Gauczynski, S., Weiss, S., Grassi, J., Rousset, M., Dormont, D. and Chambaz, J. (2005). Bovine prion is endocytosed by human enterocytes via the 37 kDa/67 kDa laminin receptor. *Am. J. Pathol.* **167**, 1033-1042.

Nunziante, M., Gilch, S. and Schatzl, H. M. (2003). Essential role of the prion protein N terminus in subcellular trafficking and half-life of PrPc. *J. Biol. Chem.* **278**, 3726-3734.

Pan, T., Wong, B. S., Liu, T., Li, R., Petersen, R. B. and Sy, M. S. (2002). Cell-surface prion protein interacts with glycosaminoglycans. *Biochem. J.* **368**, 81-90.

Parkyn, C. J., Vermeulen, E. G. M., Mootoosamy, R. C., Sunyach, C., Jacobsen, C., Oxvig, C., Moestrup, S., Liu, Q., Bu, G., Jen, A. et al. (2008). LRP1 controls biosynthetic and endocytic trafficking of neuronal prion protein. *J. Cell Sci.* **121**, 773-783.

Raman, R., Sasisekharan, V. and Sasisekharan, R. (2005). Structural insights into biological roles of protein-glycosaminoglycan interactions. *Chem. Biol.* **12**, 267-277.

Rambold, A. S., Müller, V., Ron, U., Ben-Tal, N., Winklhofer, K. F. and Tatzelt, J. (2008). Stress-protective signalling of prion protein is corrupted by scrapie prions. *EMBO J.* **27**, 1974-1984.

Schmitt-Ulms, G., Legname, G., Baldwin, M. A., Ball, H. L., Bradon, N., Bosque, P. J., Crossin, K. L., Edelman, G. M., DeArmond, S. J., Cohen, F. E. et al. (2001). Binding of neural cell adhesion molecules (N-CAMs) to the cellular prion protein. *J. Mol. Biol.* **314**, 1209-1225.

Shyng, S. L., Moulder, K. L., Lesko, A. and Harris, D. A. (1995). The N-terminal domain of a glycolipid-anchored prion protein is essential for its endocytosis via clathrin coated pits. *J. Biol. Chem.* **270**, 14793-14800.

Spielhaupter, C. and Schätzl, H. M. (2001). PrPc directly interacts with proteins involved in signalling pathways. *J. Biol. Chem.* **276**, 44604-44612.

Stuermer, C. A., Langhorst, M. F., Wiechers, M. F., Legler, D. F. Von Hanwehr, S. H., Guse, A. H. and Plattner, H. (2004). PrPc capping in T cells promotes its association with the lipid raft proteins reggie-1 and reggie-2 and leads to signal transduction. *FASEB J.* **18**, 1731-1733.

Sunyach, C., Jen, A., Deng, J., Fitzgerald, K. T., Frobert, Y., Grassi, J., McCaffrey, M. W. and Morris, R. (2003). The mechanism of internalisation of glycosylphosphatidylinositol-anchored prion protein. *EMBO J.* **22**, 3591-3601.

Taylor, D. R., Watt, N. T., Perera, W. S. S. and Hooper, N. M. (2005). Assigning functions to distinct regions of the N-terminus of the prion protein that are involved in its copper-stimulated, clathrin-dependant endocytosis. *J. Cell Sci.* **118**, 5141-5153.

Vanhoof, G., Goossens, F., De Meester, I., Hendriks, D. and Scharpé, S. (1995). Proline motifs in peptides and their biological processing. *FASEB J.* **9**, 736-744.

Vincent, B., Paitel, E., Saftig, P., Frobert, Y., Hartmann, D., De Strooper, B., Grassi, J., Lopez-Perez, E. and Checler, F. (2001). The disintegrins ADAM10 and TACE contribute to the constitutive and phorbol ester-regulated normal cleavage of the cellular prion protein. *J. Biol. Chem.* **276**, 37743-37746.

Warner, R. G., Hundt, C., Weiss, S. and Turnbull, J. E. (2002). Identification of the heparan sulfate binding sites in the cellular prion protein. *J. Biol. Chem.* **277**, 18421-18430.

Watt, N. T., Taylor, D. R., Gillott, A., Thomas, D. A., Perera, W. S. S. and Hooper, N. M. (2005). Reactive oxygen species-mediated β-cleavage of the prion protein in the cellular response to oxidative stress. *J. Biol. Chem.* **280**, 35914-35921.

Watt, N. T., Routledge, M. N., Wild, C. P. and Hooper, N. M. (2007). Cellular prion protein protects against reactive-oxygen-species-induced DNA damage. *Free Radic. Biol. Med.* **43**, 959-967.

Wopfner, F., Weidenhöfer, G., Schneider, R. von Brunn, A., Gilch, S., Schwarz, T. F., Werner, T. and Schätzl, H. M. (1999). Analysis of 27 mammalian and 9 avian PrPs reveals high conservation of flexible regions of the prion protein. *J. Mol. Biol.* **289**, 1163-1178.

Yadavalli, R., Guttmann, R. P., Seward, T., Centers, A. P., Williamson, R. A. and Telling, G. C. (2004). Calpain-dependent endoproteolytic cleavage of PrPsc modulates scrapie prion propagation. *J. Biol. Chem.* **279**, 21948-21956.

Yin, S., Yu, S., Li, C., Wong, P., Chang, B., Xiao, F., Kang, S. C., Yan, H., Xiao, G., Grassi, J. et al. (2006). Prion proteins with insert mutations have altered N-terminal conformation and increased ligand binding and are more susceptible to oxidative attack. *J. Biol. Chem.* **281**, 10698-10705.

Yin, S., Pham, N., Yu, S., Li, C., Wong, P., Chang, B., Kang, S. C., Biasini, E., Tien, P., Harris, D. A. et al. (2007). Human prion proteins with pathogenic mutations share common conformational changes resulting in enhanced binding to glycosaminoglycans. *Proc. Natl. Acad. Sci. USA* **104**, 7546-7551.

Zeng, F., Watt, N. T., Walmsley, A. R. and Hooper, N. M. (2003). Tethering the N-terminus of the prion protein compromises the cellular response to oxidative stress. *J. Neurochem.* **84**, 480-490.